

# Osteoarthritis and Cartilage



## Modeling of signaling pathways in chondrocytes based on phosphoproteomic and cytokine release data

I.N. Melas<sup>†‡b</sup>, A.D. Chairakaki<sup>†ab</sup>, E.I. Chatzopoulou<sup>†b</sup>, D.E. Messinis<sup>†‡</sup>, T. Katopodi<sup>†</sup>, V. Pliaka<sup>‡</sup>, S. Samara<sup>¶</sup>, A. Mitsos<sup>§</sup>, Z. Dailiana<sup>||</sup>, P. Kollia<sup>¶</sup>, L.G. Alexopoulos<sup>†\*</sup>

<sup>†</sup> Mechanical Engineering Department, National Technical University of Athens, Athens, Greece

<sup>‡</sup> Protatonce Ltd., Athens, Greece

<sup>§</sup> AVT Process Systems Engineering (SVT), RWTH Aachen University, Aachen, Germany

<sup>||</sup> Department of Orthopaedic Surgery, University of Thessalia, Larissa, Greece

<sup>¶</sup> Department of Genetics & Biotechnology, Faculty of Biology, National and Kapodistrian University of Athens, Athens, Greece

### ARTICLE INFO

#### Article history:

Received 29 July 2013

Accepted 7 January 2014

#### Keywords:

Modeling signaling pathways  
Signaling pathways in chondrocytes  
Phosphoproteomic signaling  
Pathway optimization

### SUMMARY

**Objective:** Chondrocyte signaling is widely identified as a key component in cartilage homeostasis. Dysregulations of the signaling processes in chondrocytes often result in degenerative diseases of the tissue. Traditionally, the literature has focused on the study of major players in chondrocyte signaling, but without considering the cross-talks between them. In this paper, we systematically interrogate the signal transduction pathways in chondrocytes, on both the phosphoproteomic and cytokine release levels.

**Methods:** The signaling pathways downstream 78 receptors of interest are interrogated. On the phosphoproteomic level, 17 key phosphoproteins are measured upon stimulation with single treatments of 78 ligands. On the cytokine release level, 55 cytokines are measured in the supernatant upon stimulation with the same treatments. Using an Integer Linear Programming (ILP) formulation, the proteomic data is combined with a priori knowledge of proteins' connectivity to construct a mechanistic model, predictive of signal transduction in chondrocytes.

**Results:** We were able to validate previous findings regarding major players of cartilage homeostasis and inflammation (e.g., IL1B, TNF, EGF, TGFA, INS, IGF1 and IL6). Moreover, we studied pro-inflammatory mediators (IL1B and TNF) together with pro-growth signals for investigating their role in chondrocytes hypertrophy and highlighted the role of underreported players such as Inhibin beta A (INHBA), Defensin beta 1 (DEFB1), CXCL1 and Flagellin, and uncovered the way they cross-react in the phosphoproteomic level.

**Conclusions:** The analysis presented herein, leveraged high throughput proteomic data via an ILP formulation to gain new insight into chondrocytes signaling and the pathophysiology of degenerative diseases in articular cartilage.

© 2014 Osteoarthritis Research Society International. Published by Elsevier Ltd. All rights reserved.

### Introduction

Articular cartilage is a connective tissue covering the ends of bones in a joint, responsible for bearing loads with minimum wear and friction. Cartilage homeostasis is orchestrated by a complex

interplay of anabolic and catabolic processes that take place in chondrocytes. Chondrocytes are meant to maintain the structure of the tissue by synthesizing collagen (mostly of type II) and proteoglycans. However in pathological situations, they release matrix metalloproteinases (MMPs) that degrade the collagen content of the tissue, leading to loss of its structural integrity. Protein signaling plays a central role to chondrocytes capability to either synthesize cartilage and maintain its homeostasis, or degrade cartilage and promote the inflammatory response seen in pathologic situations. For example, up-regulation of the SOX9 transcription factor induced by TGFB or FGF stimulation leads to collagen synthesis. On the other hand, over-activation of NFkB induced by several pathways (e.g., Inflammation related pathways or bone development

\* Address correspondence and reprint requests to: L.G. Alexopoulos, Mechanical Engineering Department, National Technical University of Athens, Athens, Greece.  
E-mail address: [leo@mail.ntua.gr](mailto:leo@mail.ntua.gr) (L.G. Alexopoulos).

<sup>a</sup> Current address: Division of Immunogenetics, Center of Immunology and Transplantation, Biomedical Research Foundation of the Academy of Athens, Athens, Greece.

<sup>b</sup> Contributed equally to this work.

processes<sup>1–7</sup>) leads to the release of MMPs and collagen degradation. Thus, chondrocytes have the potential for both anabolic and catabolic roles in articular cartilage, and the role they eventually assume is the one dictated by their signaling mechanisms as a response to their biochemical microenvironment.

The importance of protein signaling in cartilage homeostasis has been interrogated before, with most of the studies focusing on the deconvolution of signaling processes in chondrocytes and the identification of catabolic mediators. Traditionally, most of these approaches revolve around few major pathways (such as IL1A/B, TNFA, TGFA/B, etc.), without taking into account other less known players. Considering that chondrocyte function and response results as an aggregate of numerous processes and that even the slightest crosstalk can eventually affect cell behavior, the systematic study of chondrocytes signaling is of the utmost importance for uncovering the etiology of degenerative diseases and facilitate the development of novel therapies<sup>8–11</sup>. To this end, high throughput proteomic measurements combined with computational modeling offer a promising solution. Proteomics technologies allow the multiplexed quantification of proteins, while computational modeling post-processes the results in a way that interpretable conclusions can be extracted for the interrogated system.

Proteomics have been used in the study of degenerative diseases of cartilage in the past, addressing mostly the following: (1) direct analysis of cartilage protein content<sup>12–15</sup>, (2) analysis of cartilage related biological fluids<sup>16,17</sup> (Synovial fluid) and (3) study of chondrocytes secretion upon treatment with catabolic mediators<sup>18,19</sup>. In more detail, proteomic analysis of cartilage explants and chondrocytes has lead to the identification of hundreds of proteins in articular cartilage, as well as characterization of their expression patterns in normal (control) and disease patients. Findings of this analysis lead to better understanding of the etiology underlying degenerative diseases and potential drug targets. Study of chondrocyte secretory behavior may lead to deeper understanding of the cells' plasticity to mount and overcome an inflammatory response; while proteomic analysis of the synovial fluid and plasma has identified proteins differentially regulated in normal and disease patients, and aims mostly at biomarker discovery.

The applications of proteomics mentioned above, form the basis towards a systems-level understanding of the processes taking place in chondrocytes; however, they do not interrogate their signaling mechanisms. To study chondrocytes signaling, phosphoproteomic data must also be incorporated and by implementing a mathematical formalism to model how signal propagates from one protein to the next, construct predictive models of their function.

In this paper, we interrogate the signal transduction mechanisms of primary chondrocytes on both the phosphoproteomic and the cytokine release levels upon stimulation with 78 ligands, including some major players of osteoarthritic pathophysiology, as well as ligands well characterized for promoting inflammation in other cells types. Our approach is two-fold. On the experimental front we use the xMAP technology to measure the activation level of 17 key phosphoproteins and the release of 55 cytokines in the cells' supernatant, upon stimulation with single treatments of the 78 ligands. Even though the xMAP technology does not provide for signal multiplexability as high as other proteomic technologies, fast turnaround times using the Luminex equipment and low requirements in protein content allows the design of the experiment on 96-well plates, leading to high sample-throughput<sup>20,21</sup>. On the computational front, an Integer Linear Programming (ILP) formulation is used to fit a prior knowledge network (PKN) to the proteomic data, resulting in a mechanistic model, predictive of the function and response of human chondrocytes<sup>22</sup>. The proposed ILP approach is based on Boolean logic to model signal transduction in the network. Boolean logic assumes protein activation can take

only binary values (ON/OFF) and then uses Boolean gates (AND/OR/NOT) to model protein connectivity in the signaling network. By adopting Boolean logic and using a PKN – obtained from literature citations of signaling reactions – as a scaffold, we construct an initial model of the signal transduction network. Subsequently, the ILP formulation is used to train this model to the proteomic data, by removing reactions that contradict the data at hand. In this manner, the optimized model best captures the signaling patterns of human chondrocytes.

## Methods

### *Chondrocyte isolation, culture and stimulation*

Cartilage tissue was obtained from the femoral heads of patients undergoing total hip arthroplasty because of subcapital femoral fractures. Tissue was isolated using standard methods. Chondrocytes were isolated by sequential enzymatic digestion with pronase for 15 min at 37°C and 0.4% collagenase Type II for 4 h at 37°C as previously reported<sup>23</sup>. Enzymes were diluted in serum-free Dulbecco's modified Eagle's medium supplemented with 50 µg/ml gentamycin, 100 µg/ml Kanamycin and 1.25 µg/ml Fungizone Amphotericin B. Isolated chondrocytes were washed, strained with 70 µm nylon meshes, and finally seeded at high-density (50,000 cells/well) in 96-well plates resuspended in DMEM high glucose, supplemented with 10% FBS, 100 U/ml Penicillin Streptomycin, 10 mM HEPES and 1% MEM Non-essential Amino Acids Solution. Cells were cultured for 24 h (60% confluency) and were then starved overnight at 37°C, 5% CO<sub>2</sub>, in serum-free DMEM high glucose; stimulated with single treatments of 78 ligands (see [Supplementary Material 1](#)) and were finally lysed at 5 and 25 min after stimulation. The lysates were pooled in a 1:1 ratio before executing the Luminex assay. The library of 78 ligands was compiled to include some (but not all) of the major players of cartilage biology together with many underreported ligands, in an attempt to discover new players of cartilage pathophysiology.

Samples from various donors were used for developing the experimental protocols and for preliminary studies. However, the computational analysis that follows requires minimum biological variation for maximum signal to noise ratio; thus, for the final experiment only samples from a single donor were considered. We expect donor to donor variability, but that should be in the same levels as with previous studies<sup>21</sup>.

### *Luminex assay*

#### *Phosphoproteins*

A Luminex 200 system was used, to measure the activation of 17 phosphoproteins (AKT, JUN, CREB, ERK, GSK3, HISTH3, HSP27, IKB, IRS1S, JNK, MAP2K1, MAPK14, TP53, RPS6KB1, RPS6KA1, STAT3, STAT6) 5 and 25 min after stimulation, as described in<sup>21</sup>. The 17 phosphoproteins were chosen based on assay availability and quality controls performed at early stages of the experimental setup.

#### *Cytokine releases*

A library of 55 cytokine releases including most major inflammatory mediators such as cytokines, chemokines, growth factors, as well as degenerative enzymes (MMPs) (CCL27, CCL11, FGF2, CSF3, CSF2, CXCL1, HGF, ICAM, IFNA2, IFNG, IL10, IL12, IL12P40, IL13, IL15, IL16, IL17, IL18, IL1B, IL1RA, IL2, IL2R, IL3, IL4, IL5, IL6, IL7, IL8, IL9, CXCL10, LIF, CCL2, CCL7, CSF1, MIF, CXCL9, CCL4L1, CCL4L2, NGF, PDGFB, CCL5, KITLG, SCGFB, CXCL 12, TNF, LTA, TNFSF 10, VCAM1, VEGF121, MMP1, MMP10, MMP13, MMP3, MMP8, MMP9) was measured in the supernatant 24 h after stimulation.

### Data normalization

Both phosphoprotein and cytokine release data are measured in fluorescent units and is dependent on the antibody pair used for detection. For instance, MAP2K1 ranged from 280 units (untreated condition) to 6500 units (under EGF), while GSK3 ranged from 500 units (untreated condition) to 1500 units. Variations such as these do not necessarily reflect that MAP2K1 is more activated than GSK3, but may be attributed to protein abundance or assay calibration issues. Consequently two challenges emerge, firstly, identifying whether a signal is activated or not, and secondly, normalizing the raw data in a way that the optimization algorithm is not biased in favor of the highest values<sup>24</sup>. Herein we implemented the normalization procedure introduced in<sup>25</sup>: We fitted the measurements of each signal to a bimodal distribution and for each datapoint, we formed the ratio of the frequencies with respect to the two modes and passed it to a hill function to map it to [0, 1]. The normalized data were used by the ILP algorithm.

### Construction and pre-processing of the PKN

A PKN was constructed downstream the 78 receptors of interest, based on literature citations of signaling reactions<sup>25</sup>. Several online databases were queried (Reactome<sup>26</sup>, PathwayCommons<sup>27</sup>, KEGG<sup>28</sup>), but most of the reactions were obtained from Ingenuity (<http://www.ingenuity.com/>). The PKN was constructed in such a manner that it includes all interrogated receptors and measured phosphoproteins.

Upon its construction, the PKN was preprocessed to remove non-observable and non-controllable parts of it according to<sup>24</sup>. Non-observable, are nodes in the pathway whose activation state cannot be inferred based on the measured phosphoproteins (i.e., Nodes, downstream of which there are no measured signals). Non-controllable are nodes whose activation state cannot be controlled by the imposed perturbations (i.e., Nodes with no upstream stimuli). Removing non-observable, non-controllable parts of the pathway facilitates the optimization process by reducing the size of the pathway.

### Optimization of signaling pathways to proteomic data via an ILP formulation

An ILP formulation was used to fit the PKN to proteomic data by removing reactions that contradict the data at hand. See also<sup>22</sup>.

Assume a signaling network  $G$  defined as a set of reactions  $i = 1, \dots, n_r$  and species  $j = 1, \dots, n_s$ . Each reaction  $i$  is described by three index sets; the set of reactants  $R_i$ , the set of inhibitors  $H_i$  and the set of products  $P_i$ ;  $R_i, H_i, P_i \subset \{1, \dots, n_s\}$ . We also define a set of experiments  $k = 1, \dots, n_e$ . In each experiment  $k$  a set of species  $I_j^k$  are perturbed with  $I_j^k \in \{0, 1\}$ ;  $j = 1, \dots, n_s$ ;  $k = 1, \dots, n_e$ .  $I_j^k = 1$  if species  $j$  in experiment  $k$  is set to active (ON);  $I_j^k = 0$  if  $j$  is not perturbed. Moreover, we define variables  $x_j^k \in \{0, 1\}$  to denote the predicted activation state of species  $j$  in experiment  $k$ .  $x_j^k = 1$  if species  $j$  is active in experiment  $k$ ;  $x_j^k = 0$  otherwise. If species  $j$  is also measured and it is found to be active in experiment  $k$ , then  $x_j^{k,m} = 1$ , else if it is found to be inactive  $x_j^{k,m} = 0$ . We also introduce variables  $z_i^k \in \{0, 1\}$ ;  $i = 1, \dots, n_r$ ;  $k = 1, \dots, n_e$  to denote whether reaction  $i$  is active ( $z_i^k = 1$ ) or not ( $z_i^k = 0$ ) in experiment  $k$ . Finally, we define variables  $y_i \in \{0, 1\}$ ;  $i = 1, \dots, n_r$  to denote whether reaction  $i$  is present in the network.  $y_i = 1$  if reaction  $i$  is present in the network;  $y_i = 0$  otherwise.

Starting from the perturbed nodes, the signal is propagated downstream following the rules of Boolean logic. Thus,

1. A reaction  $i$  will take place in experiment  $k$  ( $z_i^k = 1$ ) if and only if it is present in the network ( $y_i = 1$ ), all reactants are present (i.e.,  $x_j^k = 1$ ;  $\forall j \in R_i$ ) and no inhibitors are present (i.e.,  $x_j^k = 0$ ;  $\forall j \in H_i$ ).
2. If a reaction  $i$  takes place all downstream species will be activated (i.e.,  $x_j^k = 1$ ;  $\forall j \in P_i$ ;  $k = 1, \dots, n_e$ ).
3. A species  $j$  will be active (i.e.,  $x_j^k = 1$ ) if and only if a reaction  $i$  takes place (i.e.,  $z_i^k = 1$ ) where this species is a product (i.e.,  $j \in P_i$ ); otherwise  $j$  will be inactive (i.e.,  $x_j^k = 0$ ).

The rules above may be formulated as linear constraints in the following manner:

$$\begin{aligned} x_j^k &\geq I_j^k; \quad j = 1, \dots, n_s; \quad k = 1, \dots, n_e \\ z_i^k &\leq x_j^k; \quad \forall j \in R_i; \quad i = 1, \dots, n_r; \quad k = 1, \dots, n_e \\ z_i^k &\leq 1 - x_j^k; \quad \forall j \in H_i; \quad i = 1, \dots, n_r; \quad k = 1, \dots, n_e \\ z_i^k &\geq y_i + \sum_{j \in R_i} (x_j^k - 1) - \sum_{j \in H_i} (x_j^k); \quad i = 1, \dots, n_r; \quad k = 1, \dots, n_e \\ x_j^k &\geq z_i^k; \quad \forall j \in P_i; \quad i = 1, \dots, n_r; \quad k = 1, \dots, n_e \\ x_j^k &\leq \sum_{i=1, \dots, n_r; j \in P_i} z_i^k + I_j^k; \quad j = 1, \dots, n_s; \quad k = 1, \dots, n_e \end{aligned} \quad (1)$$

The aim of the formulation is to identify the optimal values of  $y_i$  variables to minimize the mismatch between experimental data and model predictions. Additionally, because a number of solutions may exist with the same optimal objective value, the size of the solution is also minimized to harvest the one incorporating the fewest reactions see also<sup>22</sup>. Thus, the following objective function is used.

$$\sum_{j,k} a_j^k |x_j^k - x_j^{k,m}| + \sum_i \beta_i y_i \quad (2)$$

Equations (1) and (2) define an ILP, where (1) are the constraints of the formulation and (2) is the objective function to be minimized. The ILP is solved using Gurobi<sup>29</sup> under GAMS<sup>30</sup> (General Algebraic Modeling System, <http://www.gams.com/>). Finally, variables  $x_j^k$  and  $z_i^k$  may be relaxed to [0, 1] to speed up the optimization procedure without affecting the optimal solution, see<sup>22</sup>.

## Results

### Phosphoproteomic level

#### Phosphoproteomic measurements

Chondrocytes were stimulated with single treatments of 78 ligands while measuring the activation level of 17 key phosphoproteins via xMAP technology. The phosphoproteomic dataset is plotted in Fig. 1 via DataRail toolbox<sup>31</sup>. Fig. 1 is a collection of subplots representing the time course of the 17 signals from the unstimulated state to the average early response under each of the imposed ligands. The filling color in each subplot corresponds to the normalized value of the signal. Activated signals are plotted in red.

As shown in Fig. 1, a large number of stimuli raised a significant response in chondrocytes, activating at least one phosphoprotein signal. As positive control observations, well known players such as IL1B, TNF, EGF, TGFA, INS, IGF1 and IL6 responded as expected from previous studies. The pro-inflammatory mediators IL1B and TNF

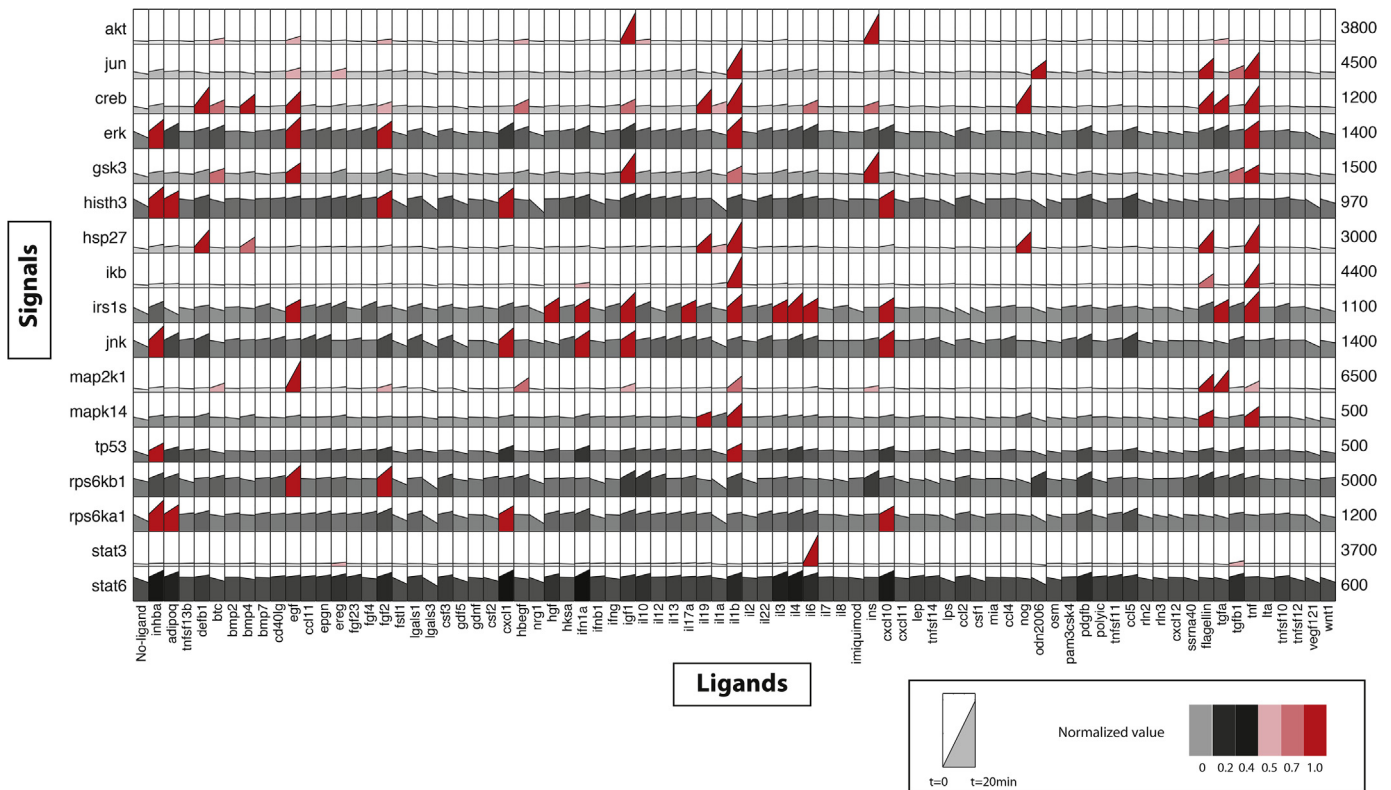


**Fig. 1.** Phosphoproteomic data: The time course of the phosphoprotein signals from the unstimulated state to the average early response is illustrated. The rows correspond to the 17 phosphoproteins measured and the columns to the 79 ligand treatments (including the No-ligand treatment). In each subplot, the first point shows the unstimulated activity of the respective signal (zero time point); the second point shows the raw measurement of the signal (in fluorescent units) 5 + 25 min after stimulation; while the color code corresponds to the normalized value (between 0 and 1) of the signal. The numbers on the right hand side of the figure show the maximum phosphorylation value of each signal in fluorescent units.

activated IKB, HSP27, MAPK14 (p38) and JUN, already known to promote inflammation in cartilage, together with pro-growth signals such as CREB, ERK, GSK3, IRS1 and MAP2K1 (MEK12), validating their role in chondrocyte hypertrophy<sup>32</sup>. On the other hand, pro-growth stimuli such as EGF, TGFA and INS activated only anabolic pathways, leaving inflammation related signals unaffected. Apart from the major players, a number of underreported stimuli are found to affect chondrocytes signaling including INHBA (Inhibin beta A), ADIPOQ (Adiponectin), DEFB1 (Defensin beta 1), BTC (Betacellulin), CXCL1, HBEGF, IL19, CXCL10, ODN2006 (Toll Like Receptor (TLR)9 ligand), NOG (Noggin) and Flagellin. A detailed description of the screened stimuli and their role in cartilage physiology is given in [Supplementary Material 1](#). See also the Discussion section.

### Pathway construction based on the ILP formulation

The ILP formulation is used to train the PKN to the phosphoproteomic data of [Fig. 1](#), resulting in an integrative model, predictive of the signal transduction mechanisms of human chondrocytes. In more detail, the formulation removed all reactions from the PKN that contradicted the data at hand in an attempt to minimize the difference between model predictions and experimental data. The optimized network is shown in [Fig. 2](#). With thick black edges we plotted the reactions that are validated by the data and with gray edges the reactions that contradicted the data and were removed by the ILP algorithm. An in depth analysis of the ILP performance and experimental validation of model predictions in the neighborhood of MAPK14, HSP27 and IKB signals is shown in [Supplementary Material 2](#).

**Fig. 2** validates the key findings of **Fig. 1** and previous reports in the literature: Major inflammatory mediators such as IL1B and TNF, signal through their receptors to IKB, MAPK14, HSP27 and JUN. IL1B also activates CREB and MAP2K1 (growth related signals) *via* TRAF6, in good accordance to the phosphoproteomic data of **Fig. 1** and the literature<sup>33</sup>. Pro-growth stimuli such as TGFA, BTC, EGF, IGF1, INS and FGF2 signal through GRB2 to SOS, RAS and from there either to MAP2K1 (MEK12) *via* RAF1, or signal through PI3K to AKT and to CREB. IL6 activates mostly STAT3 *via* JAK1. On the other hand, the signaling pathways of CXCL1, HBEGF, DEFB1, Flagellin and INHBA were uncovered for the first time in chondrocytes. CXCL1, a small cytokine of the CXC family, binds to CXCR2 and activates RPS6KA1. HBEGF, a ligand of the EGFR, signals *via* the same pathways as EGF, BTC and TGFA. DEFB1, a TLR ligand, signals through TLR4 to RAC1 and from there to the MAPKs and finally activates HSP27 demonstrating pro-inflammatory action. Flagellin, also a TLR ligand, signals through TLR5 to MYD88 and then merges with the IL1 pathway activating major inflammatory signals, CREB and MAP2K1. INHBA, a ligand of the TGFBR, signals *via* the MAPKs to activate JNK and p53.

### Experimental validation of the HSP27, MAPK14, and IKB connectivity in the solution

To validate the results of the ILP formulation, we chose a neighborhood of the optimized network and performed follow up experiments; this is the neighborhood around the HSP27, MAPK14 and IKK signals. As shown in [Fig. 2](#), HSP27, MAPK14 and IKK are activated by two pathways that overlap at NIK, one originating from IL1B and Flagellin that signals via IRAK, TIFA, TRAF6 and NIK, and a



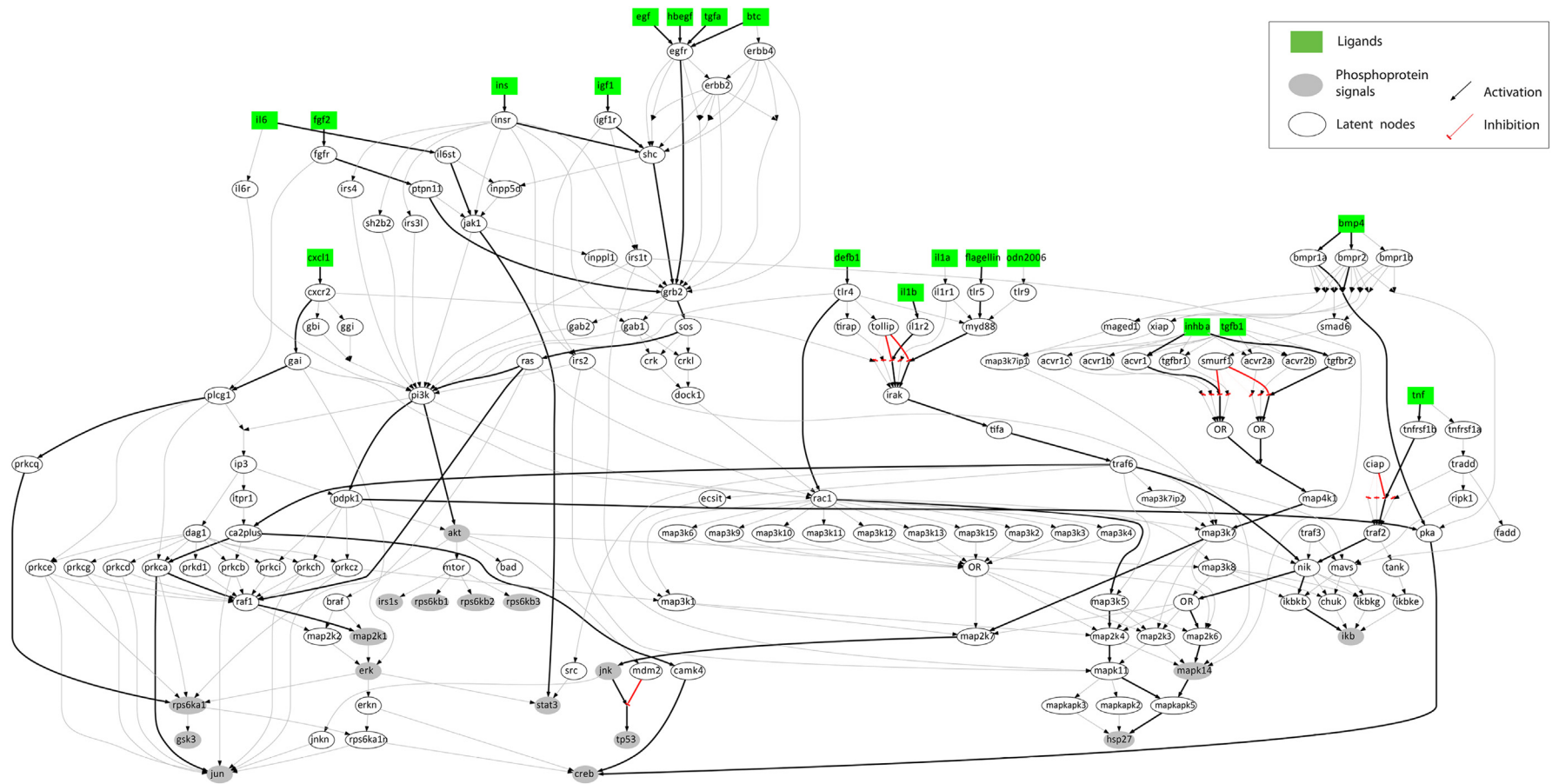


**Fig. 2.** Optimized pathway: The signal transduction network upon optimization via the ILP formulation. Green rectangular nodes correspond to the imposed ligands, gray elliptic nodes to the measured phosphoproteins, gray rectangle nodes to the measured cytokine releases and clear (white) elliptic nodes to latent signaling proteins in the network. The optimization procedure trains the PKN by removing reactions that contradict the proteomic data at hand. Thick black edges denote the reactions validated by the data; gray edges denote the reactions that contradicted the data and were removed by the ILP algorithm.

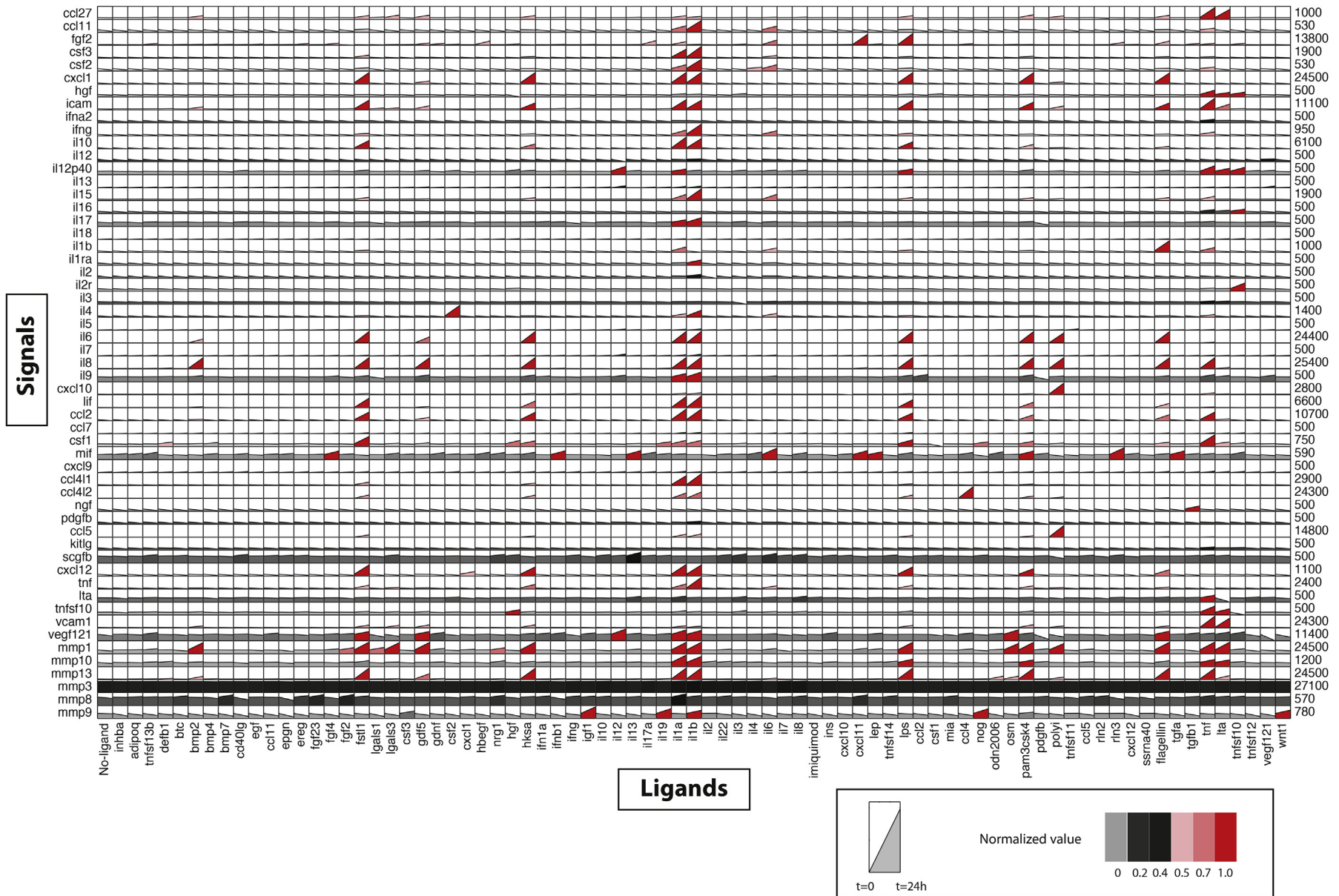


**Fig. 3.** Cytokine release data: The time course of the cytokine releases from the unstimulated state to 24 h is illustrated. The rows correspond to the 55 cytokine releases measured in the supernatant and the columns to the 79 ligand treatments (including the No-ligand treatment). In each subplot, the first point shows the unstimulated concentration of the respective cytokine in the supernatant (zero time point); the second point shows the raw measurement of the signal (in fluorescent units) 24 h after stimulation; while the color code corresponds to the normalized value (between 0 and 1) of the signal. The numbers on the right hand side of the figure show the maximum phosphorylation value of each signal in fluorescent units.

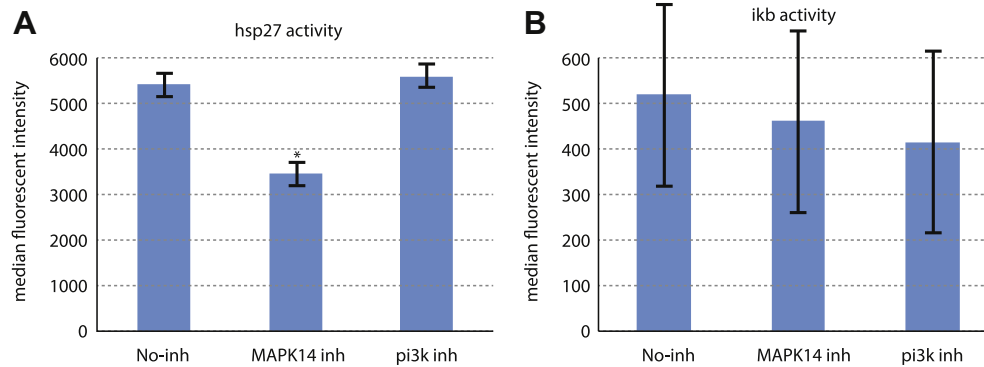


**Fig. 4.** Effects of the MAPK14 and PI3K inhibition on the activity of IKB and HSP27 upon stimulation with IL1B and TNF: Inhibition of MAPK14 clearly decreases HSP27 activity upon IL1B and TNF stimulation, validating that HSP27 is activated in a MAPK14 dependent manner, in good accordance to model predictions. IKB activity is not blocked neither by MAPK14 nor PI3K inhibition validating that IKB is activated by an independent pathway. The numbers on the left correspond to the raw phosphorylation value of the measured signals in fluorescent units.

second one originating from TNF that signals *via* TNFRSF1B, TRAF2 and NIK. Then, from NIK a pathway activates IKB *via* IKBKB and another activates MAPK14 and HSP27 *via* MAP2K6 and MAPKAPK5 (node “OR” is an auxiliary node). Note that HSP27 is downstream of MAPK14, while it is also activated by an independent pathway *via* MAPK11, MAP2K4, MAP3K5 and RAC1, but this pathway is only functional under the DEFB1 stimuli. For the rest of the stimuli (IL1B, Flagellin, TNF), HSP27 is activated *via* MAPK14.

As a follow up experiment we perturbed the cells with major activators of HSP27, MAPK14 and IKB signals, in combination with small molecular inhibitors to block key signaling proteins, while monitoring HSP27 and IKB activation in an attempt to validate the connectivity of these three nodes in the solution. As activators we used IL1B and TNF. (1) IL1B to stimulate the first pathway to NIK and (2) TNF to stimulate the second pathway to NIK as described above. As inhibitors we used a potent MAPK14 inhibitor (PHA-818637 at 100 nM) and a PI3K inhibitor (PI-103 at 10  $\mu$ M). The activation of HSP27 and IKB was measured at three time points (5, 15 and 25 min), using the Luminex xMAP technology as described in the Methods section. Results are plotted in Fig. 4.

Fig. 4(A) shows how the inhibition of MAPK14 affects HSP27. In good accordance to model predictions, inhibition of MAPK14 caused a significant decrease of HSP27 activation, since the ILP placed the HSP27 signal directly downstream of MAPK14. Note that in the initial network (gray edges in Fig. 2) a number of alternative pathways are included for HSP27 activation upon stimulation with IL1B and TNF that do not go through MAPK14 (e.g., IL1B  $\rightarrow$  IL1R2  $\rightarrow$  IRAK  $\rightarrow$  TIFA  $\rightarrow$  TRAF6  $\rightarrow$  MAP3K5  $\rightarrow$  MAP2K4  $\rightarrow$  MAPK11  $\rightarrow$  MAPKAPK5  $\rightarrow$  HSP27, or TNF  $\rightarrow$  TNFRSF1B  $\rightarrow$  TRAF2  $\rightarrow$  NIK  $\rightarrow$  MAP2K3  $\rightarrow$  MAPK11  $\rightarrow$  MAPKAPK5  $\rightarrow$  HSP27), however, these were removed by the ILP algorithm as non-functional in the interrogated cell type, and HSP27 was placed directly downstream of MAPK14. On the other hand, the inhibition of PI3K had no effects on HSP27 activation, also in good accordance to model predictions, where the MAPK14, HSP27 and IKB pathway is completely disconnected from PI3K. Finally, Fig. 4(B) shows how IKB activity is affected by MAPK14 and PI3K inhibition. In good accordance to model predictions, IKB is not affected by either MAPK14 or PI3K inhibition, since IKB is regulated by a different pathway than MAPK14 and is also disconnected from PI3K. Thus, the follow up experiments of Fig. 4 validate the connectivity of HSP27, MAPK14 and IKB in the optimized network.

#### Cytokine release level

Chondrocytes were stimulated with single treatments of 78 ligands while measuring the release of 55 cytokines. The cytokine

release data is shown in Fig. 3. Fig. 3 is a collection of subplots representing the time course of the 55 signals from the unstimulated state to 24 h, for each of the imposed ligands. The filling color in each subplot corresponds to the normalized value of the signal.

As shown in Fig. 3, a large number of the imposed stimuli promoted significant cytokine release in chondrocytes. The strongest inducers were FSTL1 (a TLR 6/2 agonist), GDF5, HKSA (TLR2 ligand), IL1A, IL1B, IL6, LPS, PAM3CSK4 (TLR 1/2 agonist), POLYIC (TLR3 agonist), Flagellin (TLR5 agonist), TNF and LTA (a member of the TNF superfamily). Most of them have already been proven to exhibit pro-inflammatory action; however, there are a number of underreported players such as GDF5 and LTA. As positive controls, we observe that major inflammatory mediators such as IL1A and IL1B raised an extensive inflammatory response inducing the release of most of the measured cytokines. Moreover, IL1A, IL1B together with many of the inflammatory mediators mentioned above were found to induce the release of MMPs (mainly MMP13 and MMP1) known to degrade the collagen content of the tissue. Finally, we observe that pro-growth stimuli did not induce any significant cytokine releases.

#### Discussion

In this paper, we have presented a rigorous approach for the study of signal transduction in chondrocytes on a systems level. We interrogated their signaling mechanisms, downstream 78 receptors of interest, on both the phosphoproteomic and the cytokine release levels and also employed an ILP formulation to construct a predictive model of their signaling processes. On the experimental front, we adopted the xMAP technology to measure 17 key phosphoproteins and the release of 55 cytokines in the supernatant, upon stimulation with single treatments of the 78 ligands. These ligands were selected to stimulate major osteoarthritic degradation pathways. On the computational front, we implemented an optimization formulation, based on the modeling of signal transduction *via* Boolean logic, to train a PKN to the proteomic data by removing reactions that appear not to be functional in primary chondrocytes.

The analysis presented herein, was able to validate previous findings regarding major players of cartilage homeostasis and inflammation (e.g., IL1B, TNF, EGF, TGFA, INS, IGF1 and IL6); highlight the role of underreported players such as INHBA, DEFB1, CXCL1 and Flagellin in chondrocyte signaling; identify their signaling pathways, and uncover the way they cross-react in the phosphoproteomic level. Even though most of the effects of the interrogated stimuli on the measured phosphoproteins or cytokine releases have been reported before, this is the very first attempt to



our knowledge to leverage high throughput proteomic data *via* a bioinformatics approach, and identify which of the signaling pathways reported in literature are functional in primary human chondrocytes and orchestrate their response to external perturbations. On this front regarding the underreported players DEFB1 and Flagellin: We identified that DEFB1 signals *via* its receptor to RAC1, to the MAPKs and ultimately activates HSP27. Flagellin signals through TLR5 to MYD88 and then merges with the IL1 pathway signaling through IRAK, TIFA, TRAF6 and activates the IKB, MAPK14 and HSP27 signals. Moreover, we were able to validate part of the DEFB1 and Flagellin pathways in the neighborhood around the MAPK14, HSP27 and IKB signals *via* an independent follow up experiment (see [Supplementary Material 2](#)), proving the predictive power of the proposed ILP algorithm and reliability of model predictions. On the other hand, the lack of data in the remaining part of these pathways implies the ambiguity of the solution from the TLRs to the neighborhood of MAPK14, HSP27 and IKB, requiring tedious follow up experiments to validate that exceeds the scope of this work. Below we discuss our findings in the context of degenerative diseases such as osteoarthritis (OA).

### Inflammatory mechanisms

OA has a strong inflammatory component<sup>4</sup>. Our analysis of cytokine release data (see [Fig. 3](#)) extensively validates the role of chondrocytes in inflammation: In [Fig. 3](#), chondrocytes are found to release cytokines and MMPs upon stimulation with major inflammatory mediators (IL1B and TNF), in good accordance to literature reports; but also upon stimulation with underreported ligands. Moreover, taking into account that the tissues used for our analysis came from healthy donors, our findings suggest even healthy cells have the potential to demonstrate a strong inflammatory response (rather than protective). In this manner, the generation of an inflammatory environment in the joint is facilitated and given that cartilage is an avascular tissue, lacking important anti-inflammatory components of peripheral blood<sup>34</sup>, this environment is sustained, eventually leading to the degradation of the tissue.

The inflammatory mechanisms of chondrocytes were also studied on the phosphoproteomic level. Using an ILP formulation<sup>22</sup>, for the first time we were able to identify the signaling pathways of underreported pro-inflammatory mediators such as DEFB1 and Flagellin (TLR ligands). Even though the role of TLR in cartilage inflammation has been studied before, this is the first attempt to identify the signaling events that lead to the up-regulation of NFkB, HSP27 and other pro-inflammatory signals upon stimulation of the TLR. In more detail, two major inflammatory pathways were uncovered: the first activating IKB *via* NIK, and the second activating HSP27 *via* MAPK11 and MAPK14 dependent mechanisms. Moreover, cross-talks of the TLR with other major inflammatory and pro-growth pathways were uncovered.

### Chondrocyte hypertrophy and proliferation

During OA, proliferation and hypertrophic differentiation of chondrocytes occur. These processes resemble to skeletal development by endochondral ossification mechanisms<sup>35</sup>. They refer to the gradual differentiation of chondrocytes and subsequent release of BMPs that leads to matrix remodeling. Our analysis of the phosphoproteomic data sheds light into these mechanisms. As seen in [Fig. 1](#), stimulation with IL1B and Flagellin (two major inflammatory mediators) apart from up-regulation of inflammatory signals, also leads to over-activation of CREB and MAP2K1, two growth related signals that are connected to hypertrophy<sup>36,37</sup> (IL1B also activates ERK, GSK3 and IRS1 but this is not shown in the network).

The mechanism of CREB and MAP2K1 activation was uncovered by the ILP algorithm and is shown in the network of [Fig. 2](#). IL1B and Flagellin signal through overlapping pathways to IRAK, TIFA and then to TRAF6. From TRAF6 either activate pro-inflammatory signals, or go through RAC1 to activate CREB and MAP2K1.

Moreover, inspection of the cytokine release data of [Fig. 3](#) reveals another potential mechanism IL1B and Flagellin induce chondrocyte hypertrophy: Both IL1B and Flagellin induce the release of FGF2 known to play a role in endochondral ossification<sup>35</sup> and CXCL1, a chemokine that induces chondrocyte hypertrophy<sup>38,39</sup>. IL1B additionally induces the release of CSF3 (another pro-growth factor). Thus, IL1B and Flagellin apart from directly activating pro-growth signals *via* the pathways discussed above, also lead to the release of pro-growth cytokines, facilitating chondrocyte hypertrophy and bone ossification indirectly.

### Innate immune response in OA TLR signaling

The role of TLR signaling in OA is becoming of increasing significance as the community attempts to identify the etiology underlying the pathogenesis of the disease. TLRs belong to the family of pattern-recognition receptors and play a pivotal role in the activation of the innate immune system in response to invading microbial components<sup>40</sup>. TLR stimulation elicits strong release of pro-inflammatory cytokines<sup>41</sup>; while only recently human articular chondrocytes were shown to express TLRs<sup>42,43</sup>. In this paper we addressed TLR signaling extensively by screening 10 TLR ligands (DEFB1, HKSA, Imiquimod, Flagellin, LPS, ODN2006, PAM3CSK4, POLYIC, SSRNA40 and FSTL1). On the cytokine release level 6 of them (FSTL1, HKSA, LPS, PAM3CSK4, POLYIC and Flagellin) were found to raise a strong inflammatory response, validating the significance of TLR stimulation in joint inflammation. However, on the phosphoproteomic level only DEFB1 and Flagellin signaled through pathways monitored by the 17 phosphoprotein signals. DEFB1 signaled *via* TLR4 to RAC1 and from there to the MAPKs, eventually activating HSP27. Flagellin signaled *via* a pathway overlapping with IL1B and as discussed above, activated most inflammatory signals together with MAP2K1 and CREB.

Overall, the proposed approach successfully addressed the construction of a predictive model of the signaling mechanisms in human chondrocytes. We interrogated signal transduction on both the phosphoproteomic and cytokine release levels, upon stimulation with 78 factors of interest, including most major players of osteoarthritic pathophysiology, as well as ligands important for other cell types. Our analysis validated previous findings in chondrocytes signaling, elucidated the role of underreported players and identified cross-talks on the phosphoproteomic level, highlighting the pleiotropic role of major players in cartilage homeostasis and inflammation.

### Author contributions

LG Alexopoulos and AD Chairakaki conceived the core of this work and designed the experiments. AD Chairakaki executed the experiments. A Mitsos conceived and implemented the ILP formulation. LG Alexopoulos drafted the manuscript. IN Melas applied the ILP formulation, wrote a significant part of the manuscript and compiled the figures. DE Messinis constructed the prior knowledge network. EI Chatzopoulou and AD Chairakaki interpreted the results and wrote an important part of the manuscript. AD Chairakaki wrote the [Supplementary Material 1](#). T Katopodi, V Pliaka and S Samara designed, executed and interpreted the follow up experiments shown in [Supplementary Material 2](#). Z Dailiana performed the surgical procedures, obtained the tissue samples



and interpreted the results. P Kollia interpreted the results. All authors edited and approved the final version of the manuscript.

#### Role of the funding source

This work was funded by European Social Fund (ESF) and Greek national funds through the Operational Program Education and Lifelong Learning of the National Strategic Reference Framework (NSRF) – Research Funding Program: ERC.

#### Conflict of interest

The authors declare no competing interests for this work.

#### Acknowledgments

We gratefully acknowledge the contribution of Danai Kirli-Florou for helping with the construction of the Prior Knowledge Network. This article was based on work funded by European Social Fund (ESF) and Greek national funds through the Operational Program Education and Lifelong Learning of the National Strategic Reference Framework (NSRF) – Research Funding Program: ERC. We also thank GUROBI OPTIMIZATION for providing GUROBI optimizer free of charge.

#### Supplementary data

Supplementary data related to this article can be found at <http://dx.doi.org/10.1016/j.joca.2014.01.001>

#### References

1. Berenbaum F. Signaling transduction: target in osteoarthritis. *Curr Opin Rheumatol* 2004;16(5):616–22.
2. Chakraborti S, Mandal M, Das S, Mandal A, Chakraborti T. Regulation of matrix metalloproteinases: an overview. *Mol Cell Biochem* 2003;253:269–85, <http://dx.doi.org/10.1023/A:1026028303196>.
3. Baldwin A. The NF-kappa B and I kappa B proteins: new discoveries and insights. *Annu Rev Immunol* 1996;14:649–83.
4. Marcu K, Otero M, Olivetto E, Borzi R, Goldring M. NF-kappaB signaling: multiple angles to target OA. *Curr Drug Targets* 2010;11(5):599613.
5. Guilak F, Fermor B, Keefe F, Kraus V, Olson S, Pisetsky D, et al. The role of biomechanics and inflammation in cartilage injury and repair. *Clin Orthop Relat Res* 2004;423:17–26.
6. Luyten FP, Tylzanowski P, Lories RJ. Wnt signaling and osteoarthritis. *Bone* 2009;44(4):522–7, <http://dx.doi.org/10.1016/j.bone.2008.12.006>.
7. Lories R, Luyten F. Bone morphogenetic proteins in destructive and remodeling arthritis. *Arthritis Res Ther* 2007;9(2):207, <http://dx.doi.org/10.1186/ar2135>.
8. Hopkins AL. Network pharmacology: the next paradigm in drug discovery. *Nat Chem Biol* 2008;4:682–90.
9. Mobasheri A. Applications of proteomics to osteoarthritis, a musculoskeletal disease characterized by aging. *Front physiology* 2011;2:108.
10. Wilson R, Whitelock JM, Bateman JF. Proteomics makes progress in cartilage and arthritis research. *Matrix Biol* 2009;28(3):121–8, <http://dx.doi.org/10.1016/j.matbio.2009.01.004>.
11. Shigemizu D, Hu Z, Hung J-H, Huang C-L, Wang Y, DeLisi C. Using functional signatures to identify repositioned drugs for breast, myelogenous leukemia and prostate cancer. *PLoS Comput Biol* 2012;8(2):e1002347, <http://dx.doi.org/10.1371/journal.pcbi.1002347>.
12. Garcia BA, Platt MD, Born TL, Shabanowitz J, Marcus NA, Hunt DF. Protein profile of osteoarthritic human articular cartilage using tandem mass spectrometry. *Rapid Commun Mass Spectrom* 2006;20(20):2999–3006, <http://dx.doi.org/10.1002/rcm.2692>.
13. Wu J, Liu W, Bemis A, Wang E, Qiu Y, Morris EA, et al. Comparative proteomic characterization of articular cartilage tissue from normal donors and patients with osteoarthritis. *Arthritis Rheum* 2007;56(11):3675–84, <http://dx.doi.org/10.1002/art.22876>.
14. Jean-Baptiste V, Frdric L, Gueorgui K, Franois G, Patrick N, Didier M, et al. Establishment of a reliable method for direct proteome characterization of human articular cartilage. *Mol Cell Proteomics* 2006;5:1984–95.
15. Lambrecht S, Verbruggen G, Verdonk P, Elewaut D, Deforce D. Differential proteome analysis of normal and osteoarthritic chondrocytes reveals distortion of vimentin network in osteoarthritis. *Osteoarthritis and Cartilage* 2008;16(2):163–73, <http://dx.doi.org/10.1016/j.joca.2007.06.005>.
16. Sinz A, Bantscheff M, Mikkat S, Ringel B, Drynda S, Kekow J, et al. Mass spectrometric proteome analyses of synovial fluids and plasmas from patients suffering from rheumatoid arthritis and comparison to reactive arthritis or osteoarthritis. *Electrophoresis* 2002;23(19):3445–56, [http://dx.doi.org/10.1002/1522-2683\(200210\).23:19<3445::AID-ELPS3445>3.0.CO;2-J](http://dx.doi.org/10.1002/1522-2683(200210).23:19<3445::AID-ELPS3445>3.0.CO;2-J).
17. Liao H, Wu J, Kuhn E, Chin W, Chang B, Jones MD, et al. Use of mass spectrometry to identify protein biomarkers of disease severity in the synovial fluid and serum of patients with rheumatoid arthritis. *Arthritis Rheum* 2004;50(12):3792–803, <http://dx.doi.org/10.1002/art.20720>.
18. Catterall JB, Rowan AD, Sarsfield S, Saklatvala J, Wait R, Cawston TE. Development of a novel 2d proteomics approach for the identification of proteins secreted by primary chondrocytes after stimulation by il-1 and oncostatin m. *Rheumatology* 2006;45(9):1101–9, <http://dx.doi.org/10.1093/rheumatology/kei060>.
19. Haglund L, Bernier SM, Onnerfjord P, Recklies AD. Proteomic analysis of the lps-induced stress response in rat chondrocytes reveals induction of innate immune response components in articular cartilage. *Matrix Biol* 2008;27(2):107–18, <http://dx.doi.org/10.1016/j.matbio.2007.09.009>.
20. Saez-Rodriguez J, Alexopoulos LG, Stolovitzky G. Setting the standards for signal transduction research. *Sci Signal* 2011;4(160), <http://dx.doi.org/10.1126/scisignal.2001844>. pe10.
21. Alexopoulos LG, Saez Rodriguez J, Cosgrove BD, Lauffenburger DA, Sorger PK. Networks inferred from biochemical data reveal profound differences in toll-like receptor and inflammatory signaling between normal and transformed hepatocytes. *Mol Cell Proteomics* 2010, <http://dx.doi.org/10.1074/mcp.M110.000406>.
22. Mitsos A, Melas IN, Siminelakis P, Chairakaki AD, Saez-Rodriguez J, Alexopoulos LG. Identifying drug effects via pathway alterations using an integer linear programming optimization formulation on phosphoproteomic data. *PLoS Comput Biol* 2009;5(12):e1000591, <http://dx.doi.org/10.1371/journal.pcbi.1000591>.
23. Quinn T, Schmid P, Hunziker E, Grodzinsky A. Proteoglycan deposition around chondrocytes in agarose culture: construction of a physical and biological interface for mechanotransduction in cartilage. *Biorheology* 2002;39:27–37.
24. Saez-Rodriguez J, Alexopoulos L, Epperlein J, Samaga R, Lauffenburger D, Klamt S, et al. Discrete logic modelling as a means to link protein signalling networks with functional

- analysis of mammalian signal transduction. *Mol Syst Biol* 2009;5:331.
25. Melas IN, Mitsos A, Messinis D, Weiss T, Saez-Rodriguez J, Alexopoulos LG. Construction of large signaling pathways using an adaptive perturbation approach with phosphoproteomic data. *Mol Biosyst* 2012;8:1571–84, <http://dx.doi.org/10.1039/c2mb05482e>.
  26. Joshi-Tope G, Gillespie M, Vastrik I, D'Eustachio P, Schmidt E, de Bono B, et al. Reactome: a knowledgebase of biological pathways. *Nucleic Acids Res* 2005;33(Suppl 1):D428–32, <http://dx.doi.org/10.1093/nar/gki072>.
  27. Cerami EG, Gross BE, Demir E, Rodchenkov I, Babur, Anwar N, et al. Pathway commons, a web resource for biological pathway data. *Nucleic Acids Res* 2011;39(Suppl 1):D685–90, <http://dx.doi.org/10.1093/nar/gkq1039>.
  28. Kanehisa M, Goto S. KEGG: kyoto encyclopedia of genes and genomes. *Nucleic Acids Res* 2000;28(1):27–30, <http://dx.doi.org/10.1093/nar/28.1.27>.
  29. Gurobi I. Optimization, Gurobi Optimizer Reference Manual 2013.
  30. Brooke A, Kendrick D, Meeraus A. GAMS: User's Guide. Redwood City, California: The Scientific Press; 1988.
  31. Saez-Rodriguez J, Goldsipe A, Muhlich J, Alexopoulos LG, Millard B, Lauffenburger DA, et al. Flexible informatics for linking experimental data to mathematical models via Data-Rail. *Bioinformatics* 2008;24:840–7, <http://dx.doi.org/10.1093/bioinformatics/btn018>.
  32. Goldring MB. Chondrogenesis, chondrocyte differentiation, and articular cartilage metabolism in health and osteoarthritis. *Ther Adv Musculoskelet Dis* 2012;4(4):269–85, <http://dx.doi.org/10.1177/1759720X12448454>.
  33. Scanzello CR, Plaas A, Crow MK. Innate immune system activation in osteoarthritis: is osteoarthritis a chronic wound? *Curr Opin Rheumatol* 2008;20(5):565–72, <http://dx.doi.org/10.1097/BOR.0b013e32830aba34>.
  34. Serhan CN, Brain SD, Buckley CD, Gilroy DW, Haslett C, O'Neill LAJ, et al. Resolution of inflammation: state of the art, definitions and terms. *FASEB J* 2007;21(2):325–32, <http://dx.doi.org/10.1096/fj.06-7227rev>.
  35. Dreier R. Hypertrophic differentiation of chondrocytes in osteoarthritis: the developmental aspect of degenerative joint disorders. *Arthritis Res Ther* 2010;12(5):216, <http://dx.doi.org/10.1186/ar3117>.
  36. Long F, Schipani E, Asahara H, Kronenberg H, Montminy M. The CREB family of activators is required for endochondral bone development. *Development* 2001;128(4):541–50.
  37. Murakami S, Balmes G, McKinney S, Zhang Z, Givol D, de Crombrughe B. Constitutive activation of mek1 in chondrocytes causes stat1-independent achondroplasia-like dwarfism and rescues the fgfr3-deficient mouse phenotype. *Genes Dev* 2004;18(3):290–305, <http://dx.doi.org/10.1101/gad.1179104>.
  38. Merz D, Liu R, Johnson K, Terkeltaub R. Il-8/cxcl8 and growth-related oncogene/cxcl1 induce chondrocyte hypertrophic differentiation. *J Immunol* 2003;171(8):4406–15.
  39. Olivetto E, Vitellozzi R, Fernandez P, Falcieri E, Battistelli M, Burattini S, et al. Chondrocyte hypertrophy and apoptosis induced by GRO require three-dimensional interaction with the extracellular matrix and a co-receptor role of chondroitin sulfate and are associated with the mitochondrial splicing variant of cathepsin B. *J Cell Physiol* 2007;210(2):417–27, <http://dx.doi.org/10.1002/jcp.20864>.
  40. Medzhitov R, Preston-Hurlburt P, Janeway CAJ. A human homologue of the Drosophila toll protein signals activation of adaptive immunity. *Nature* 1997;388(6640):394–7, <http://dx.doi.org/10.1038/41131>.
  41. Kim HA, Cho M-L, Choi HY, Yoon CS, Jhun JY, Oh HJ, et al. The catabolic pathway mediated by toll-like receptors in human osteoarthritic chondrocytes. *Arthritis Rheum* 2006;54(7):2152–63, <http://dx.doi.org/10.1002/art.21951>.
  42. Su S-L, Tsai C-D, Lee C-H, Salter D, Lee H-S. Expression and regulation of toll-like receptor 2 by il-1 and fibronectin fragments in human articular chondrocytes. *Osteoarthritis and Cartilage* 2005;13(10):879–86, <http://dx.doi.org/10.1016/j.joca.2005.04.017>.
  43. Liu-Bryan R, Pritzker K, Firestein GS, Terkeltaub R. TLR2 signaling in chondrocytes drives calcium pyrophosphate dihydrate and monosodium urate crystal-induced nitric oxide generation. *J Immunol* 2005;174(8):5016–23.